

## Electronic Supplementary Information

### **Synthesis, characterization and third order nonlinear optical properties of *trans*-A<sub>2</sub>B-type cobalt corroles**

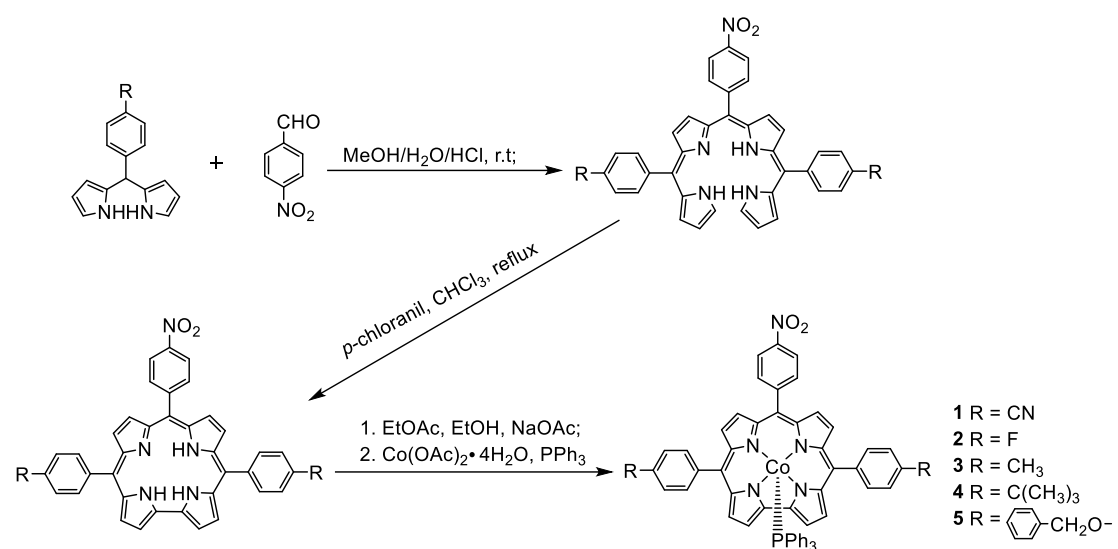
**Guifen Lu,\* Peng Zhang, Yuanyuan Fang, Yongjie Gao, Qikang Hu**

*School of Chemistry and Chemical Engineering, Jiangsu University, Zhenjiang 212013, P. R. China*

**Materials.** Reagents and solvents (Sinopharm or Aldrich) were of the highest grade available and were used without further purification, except for  $\text{CH}_2\text{Cl}_2$ , which was distilled under reduced pressure prior to use from  $\text{P}_2\text{O}_5$ . Tetra-*n*-butylammonium perchlorate (TBAP), as supporting electrolyte, was recrystallized from ethyl alcohol, and dried under vacuum at 40 °C for at least 1 week prior to use.

**Physical Measurements.** IR spectra (KBr pellets) were recorded on AVATAR-370 spectrometer.  $^1\text{H}$ NMR spectra were recorded in a  $\text{CDCl}_3$  solution at 400 MHz using a Bruker Advance 400 spectrometer at 25 °C. Chemical shifts (ppm) were determined with TMS as the internal reference. MALDI-TOF mass spectra were carried out on a Bruker BIFLEX III ultrahigh resolution Fourier transform ion cyclotron resonance (FT-ICR) mass spectrometer with  $\alpha$ -cyano-4-hydroxycinnamic acid as matrix. The fluorescence spectrum was recorded on a CaryEclipse fluorescence spectrophotometer.

**Electrochemistry.** Cyclic voltammetry was carried out at 298 K using a CHI-730C Electrochemical Workstation. A homemade three-electrode cell was used for cyclic voltammetric measurements and consisted of a glassy carbon working electrode, a platinum counter electrode and a homemade saturated calomel reference electrode (SCE). The SCE was separated from the bulk of the solution by a fritted glass bridge of low porosity which contained the solvent/supporting electrolyte mixture. All potentials are referenced to the SCE. High purity  $\text{N}_2$  was used to deoxygenate the solution and a stream of nitrogen gas was kept over the solution during each electrochemical experiment.



**Scheme S1.** Synthetic route for compounds [Cor(*p*-RPh)<sub>2</sub>(*p*-NO<sub>2</sub>Ph)]Co(PPh<sub>3</sub>) **1-5**.

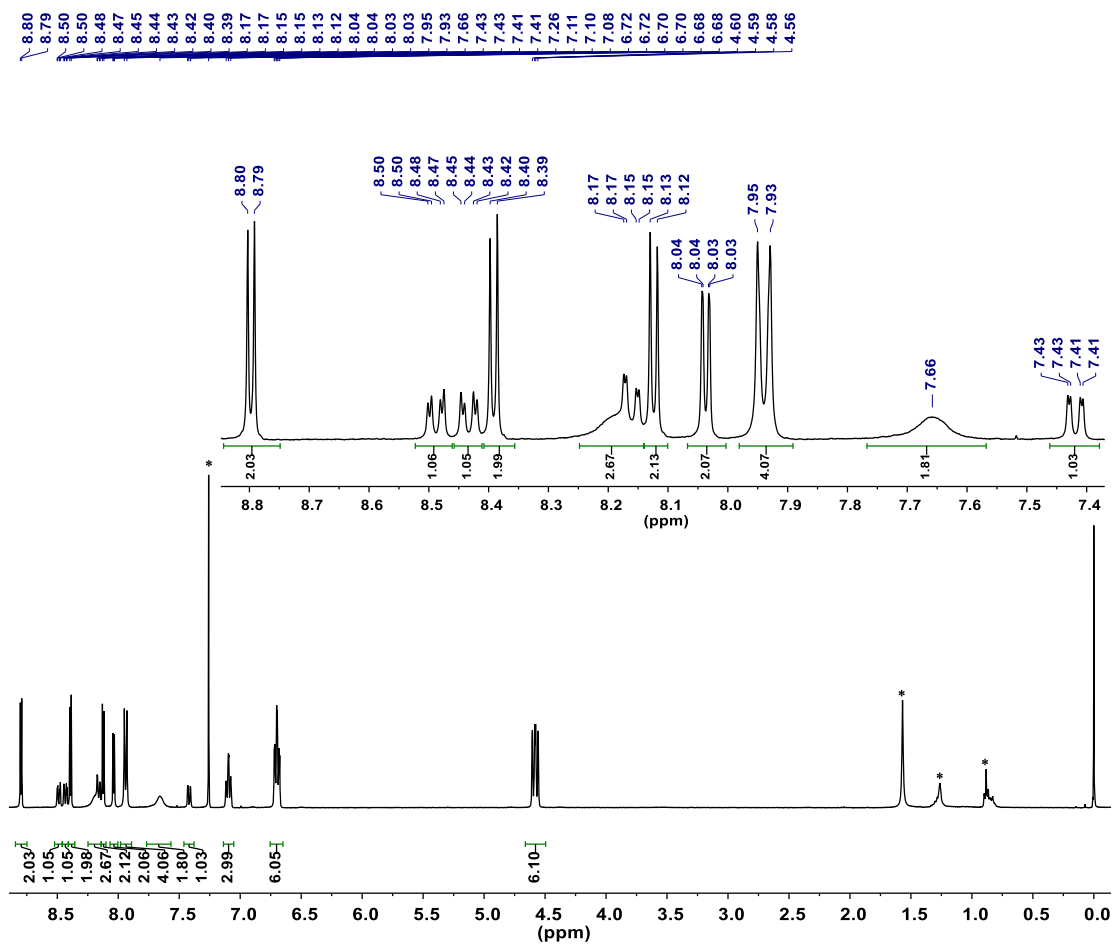


**Fig. S1.** <sup>1</sup>H NMR spectrum of [Cor(*p*-CNPh)<sub>2</sub>(*p*-NO<sub>2</sub>Ph)]Co(PPh<sub>3</sub>) (**1**) (\* 7.26 ppm is the solvent peak of CDCl<sub>3</sub>, 1.56 ppm is the peak of H<sub>2</sub>O, 0.88 and 1.26 ppm are solvent peaks from *n*-hexane).

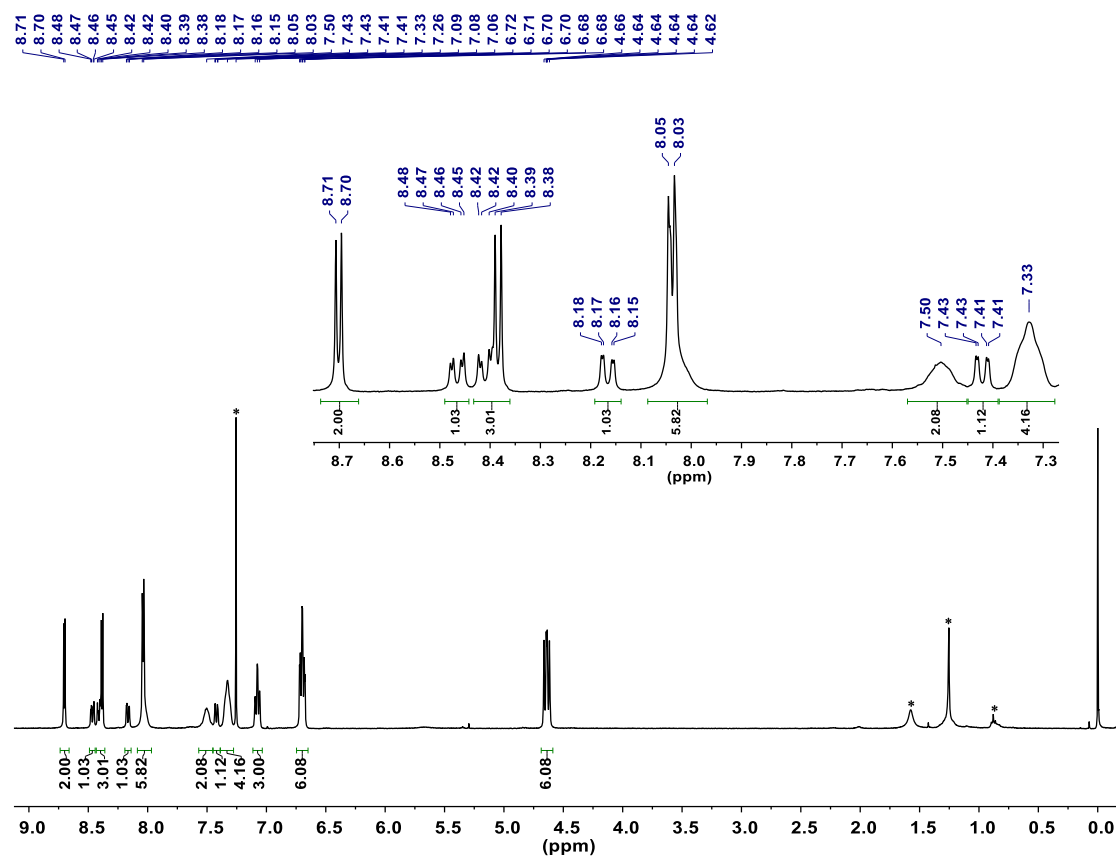


**Fig. S2.**  $^1\text{H}$  NMR spectrum of  $[\text{Co}(p\text{-FPh})_2(p\text{-NO}_2\text{Ph})]\text{Co}(\text{PPh}_3)$  (**2**) (\* 7.26 ppm is the solvent peak of  $\text{CDCl}_3$ , 1.56 ppm is the peak of  $\text{H}_2\text{O}$ , 0.88 and 1.26 ppm are solvent peaks from *n*-hexane).

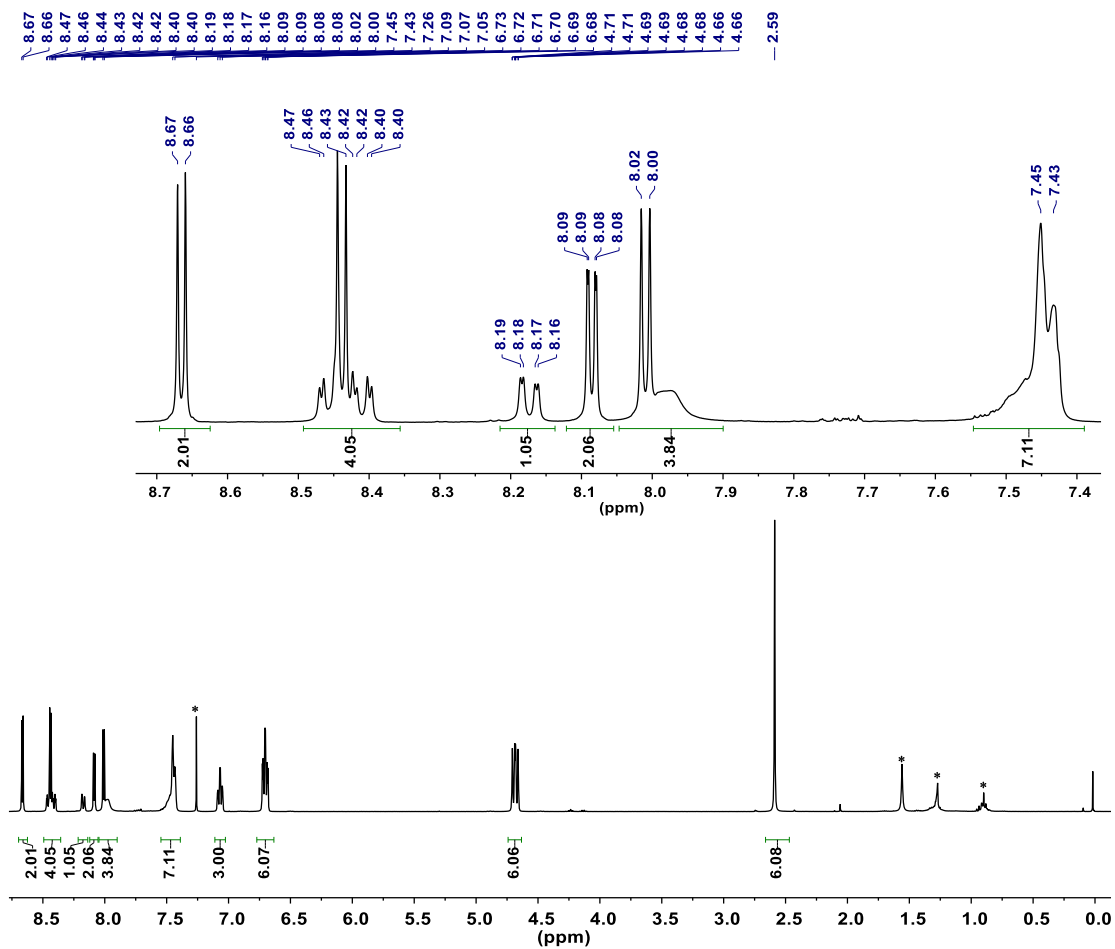


**Fig. S3.** <sup>1</sup>H NMR spectrum of [Cor(*p*-CH<sub>3</sub>Ph)<sub>2</sub>(*p*-NO<sub>2</sub>Ph)]Co(PPh<sub>3</sub>) (**3**) (\* 7.26 ppm is the solvent peak of CDCl<sub>3</sub>, 1.56 ppm is the peak of H<sub>2</sub>O, 0.88 and 1.26 ppm are solvent peaks from *n*-hexane).

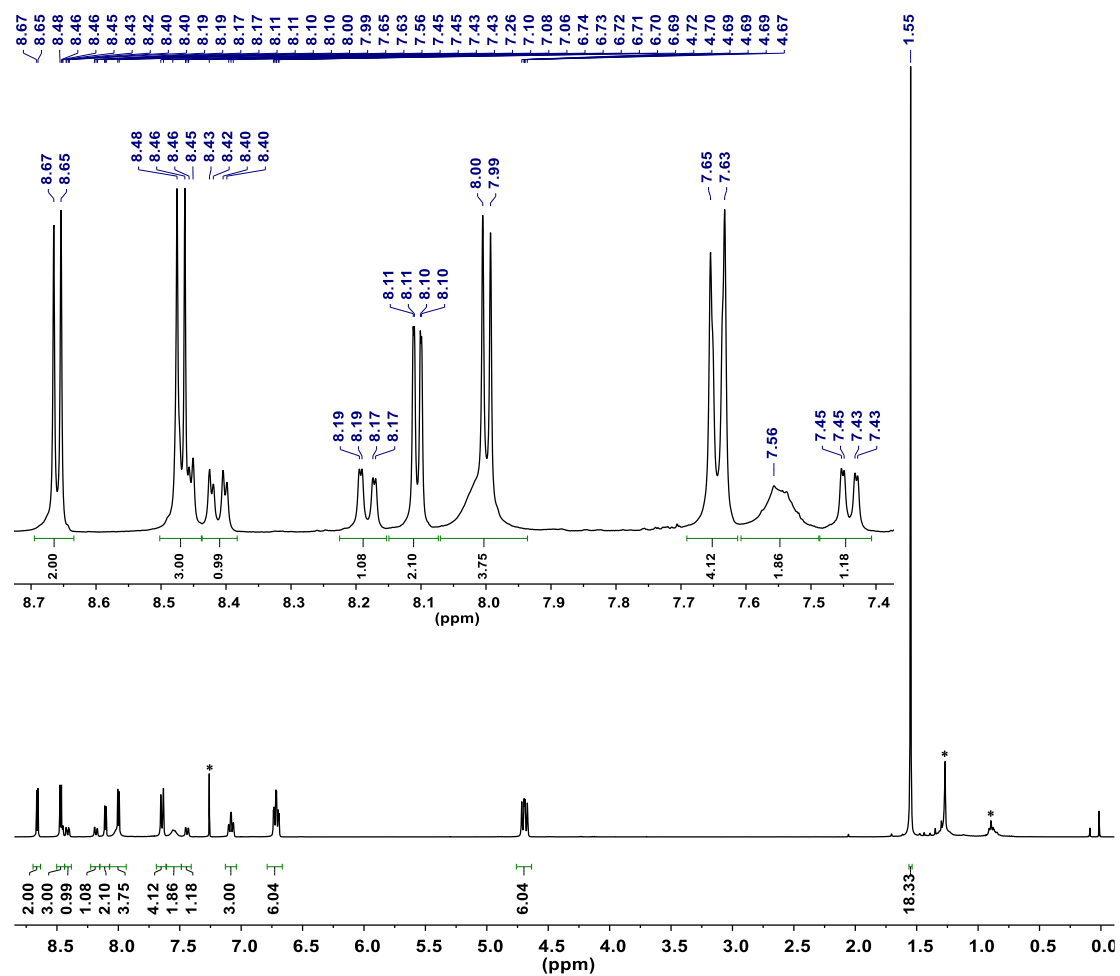


**Fig. S4.**  $^1\text{H}$  NMR spectrum of  $[\text{Co}(\text{p-C}(\text{CH}_3)_3\text{Ph})_2(\text{p-NO}_2\text{Ph})]\text{Co}(\text{PPh}_3)$  (**4**) (\* 7.26 ppm is the solvent peak of  $\text{CDCl}_3$ , 0.88 and 1.26 ppm are solvent peaks from *n*-hexane).

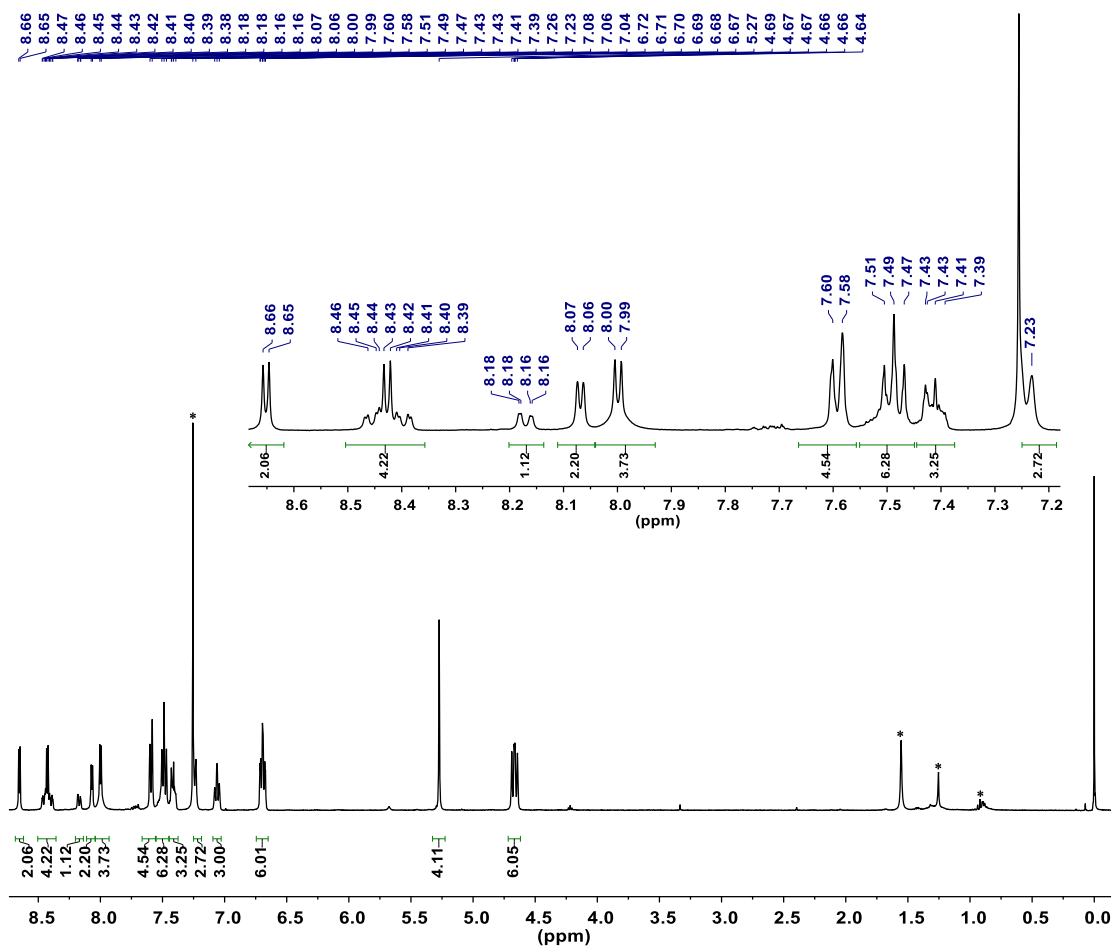


**Fig. S5.** <sup>1</sup>H NMR spectrum of [Cor(*p*-PhCH<sub>2</sub>OPh)<sub>2</sub>(*p*-NO<sub>2</sub>Ph)]Co(PPh<sub>3</sub>) (**5**) (\* 7.26 ppm is the solvent peak of CDCl<sub>3</sub>, 1.56 ppm is the peak of H<sub>2</sub>O, 0.88 and 1.26 ppm are solvent peaks from *n*-hexane).



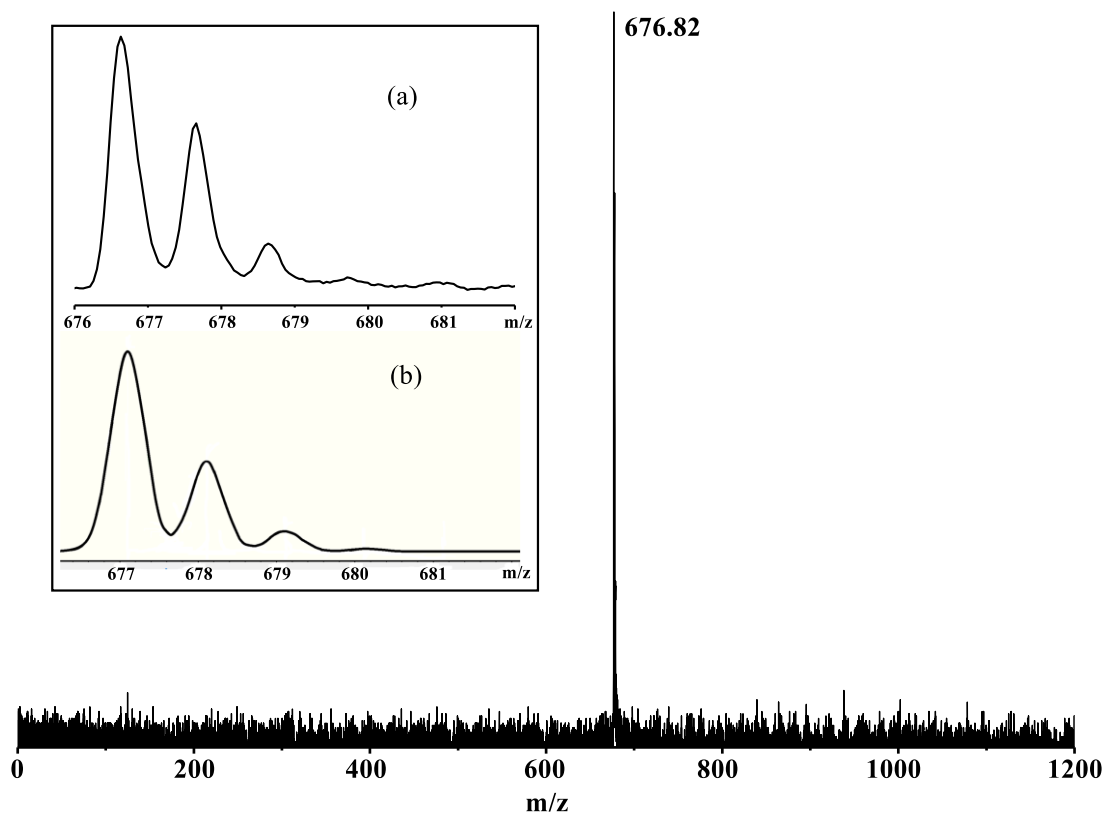


**Fig. S6.** MALDI-TOF mass spectrum of  $[\text{Co}(p\text{-CNPh})_2(p\text{-NO}_2\text{Ph})]\text{Co}(\text{PPh}_3)$  (**1**). The inset shows experimental (a) and simulated isotopic pattern (b) for the molecular ion of compound **1**.

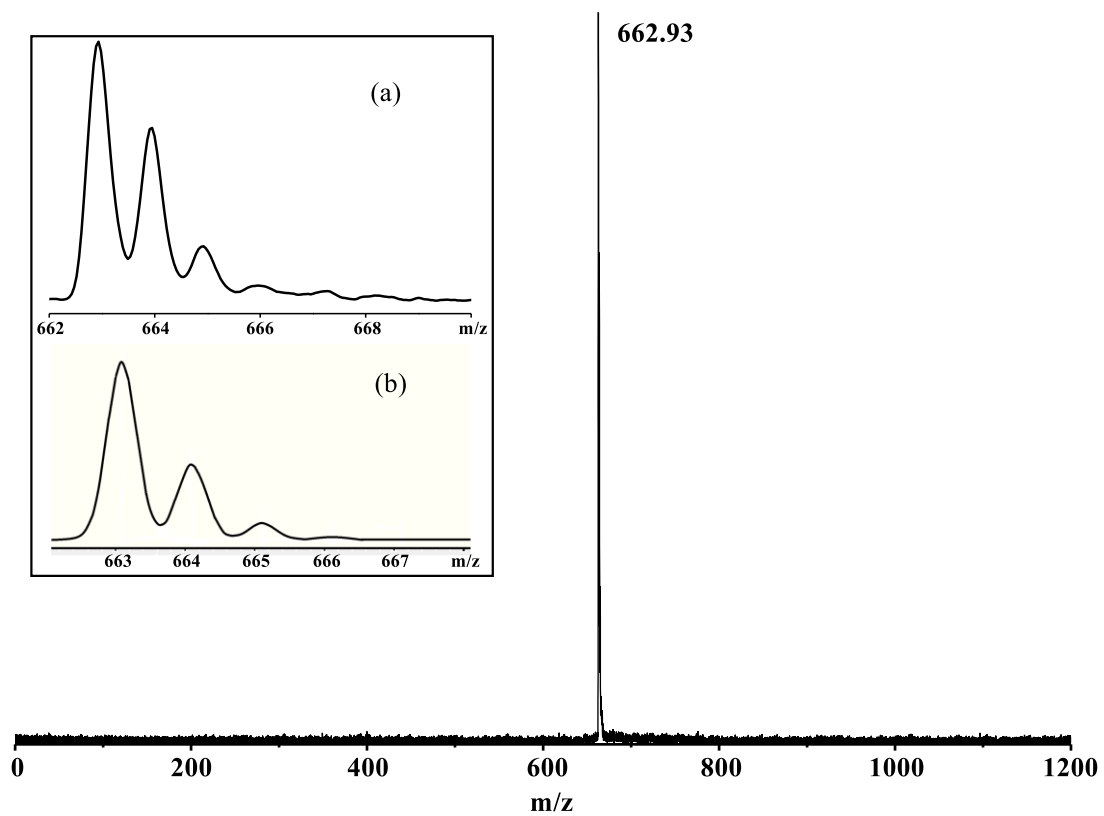


**Fig. S7.** MALDI-TOF mass spectrum of  $[\text{Co}(p\text{-FPh})_2(p\text{-NO}_2\text{Ph})]\text{Co}(\text{PPh}_3)$  (**2**). The inset shows experimental (a) and simulated isotopic pattern (b) for the molecular ion of compound **2**.

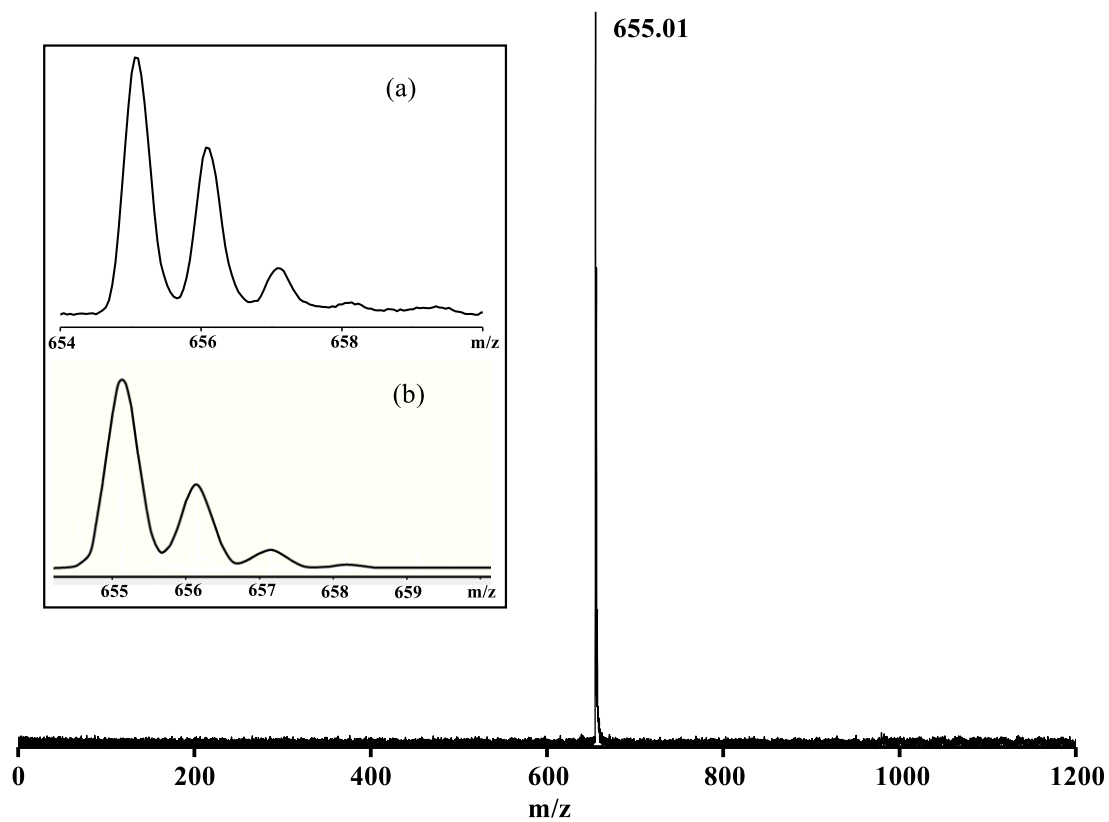


**Fig. S8.** MALDI-TOF mass spectrum of  $[\text{Co}(p\text{-CH}_3\text{Ph})_2(p\text{-NO}_2\text{Ph})]\text{Co}(\text{PPh}_3)$  (**3**). The inset shows experimental (a) and simulated isotopic pattern (b) for the molecular ion of compound **3**.

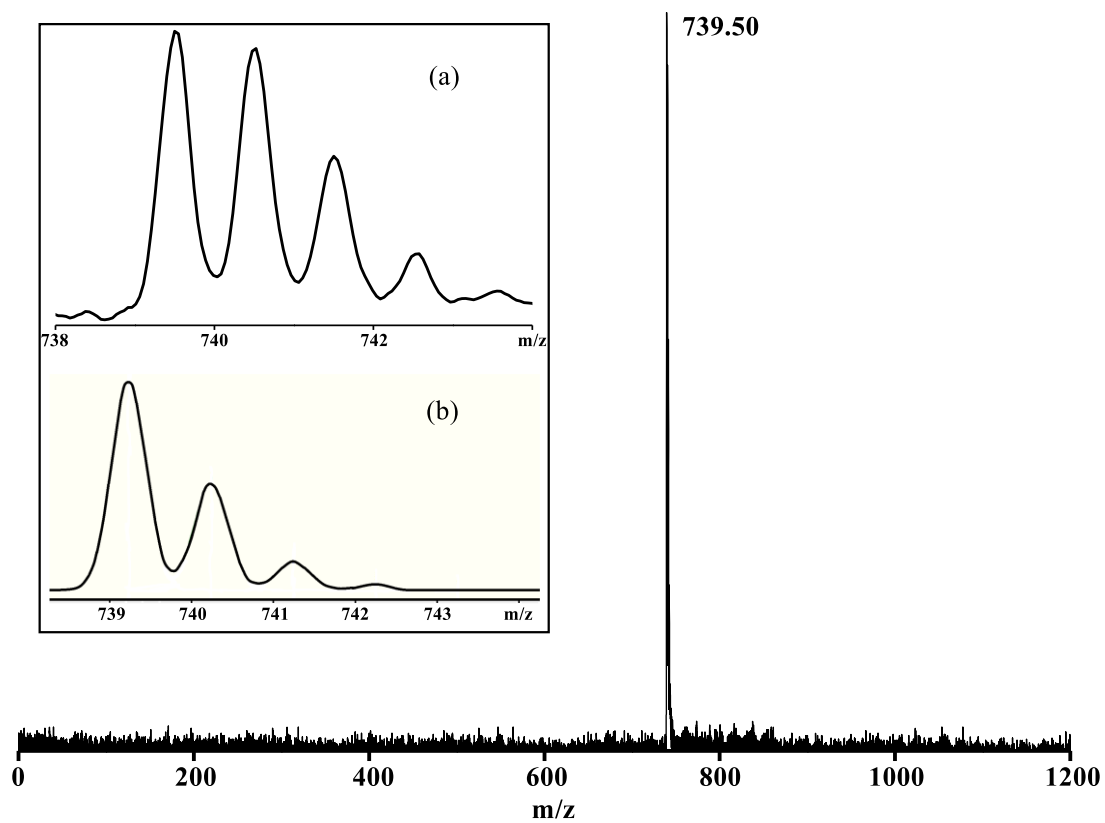


**Fig. S9.** MALDI-TOF mass spectrum of  $[\text{Co}(p\text{-C}(\text{CH}_3)_3\text{Ph})_2(p\text{-NO}_2\text{Ph})]\text{Co}(\text{PPh}_3)$  (**4**). The inset shows experimental (a) and simulated isotopic pattern (b) for the molecular ion of compound **4**.

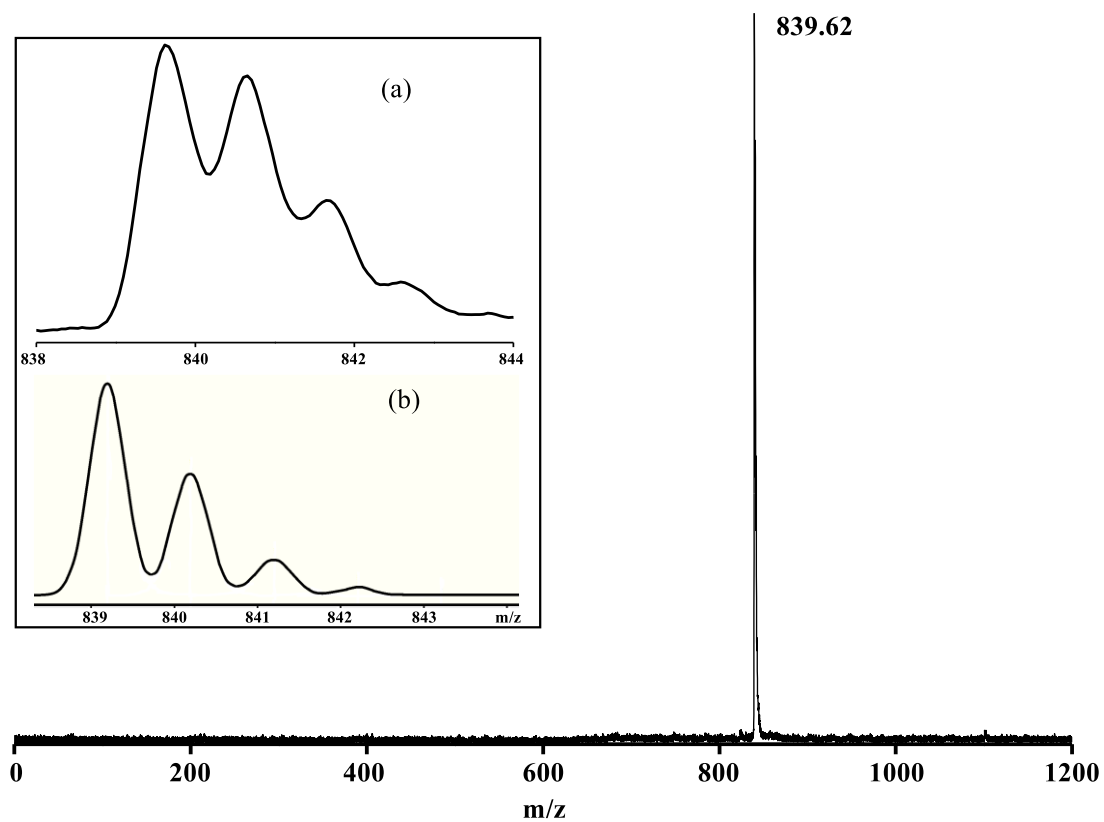


**Fig. S10.** MALDI-TOF mass spectrum of  $[\text{Co}(p\text{-PhCH}_2\text{OPh})_2(p\text{-NO}_2\text{Ph})]\text{Co}(\text{PPh}_3)$  (**5**). The inset shows experimental (a) and simulated isotopic pattern (b) for the molecular ion of compound **5**.

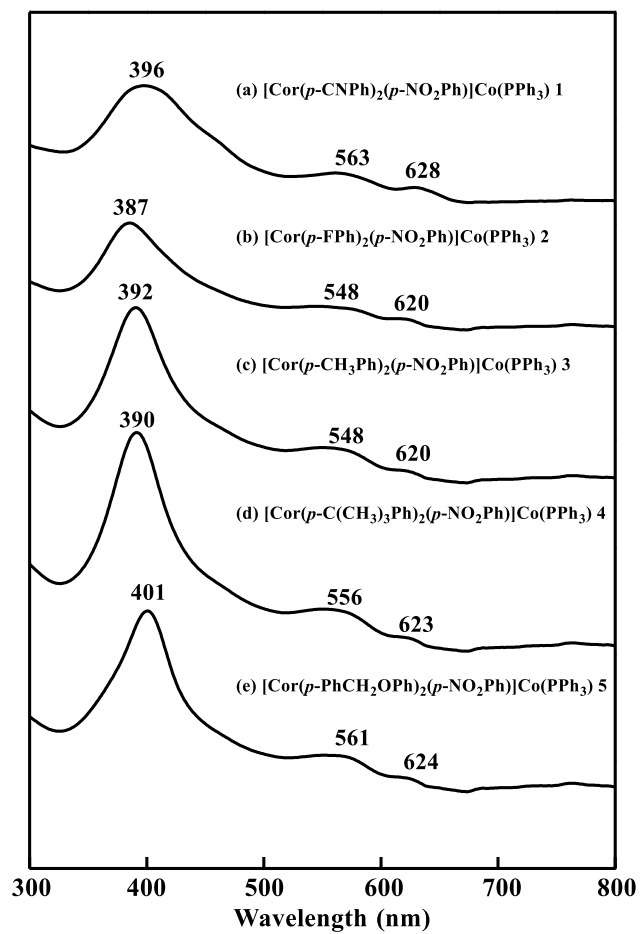


**Fig. S11.** Electronic absorption spectra of compounds  $[\text{Co}(\textit{p}\text{-RPh})_2(\textit{p}\text{-NO}_2\text{Ph})]\text{Co}(\text{PPh}_3)_3$  (**1-5**) in DMF.

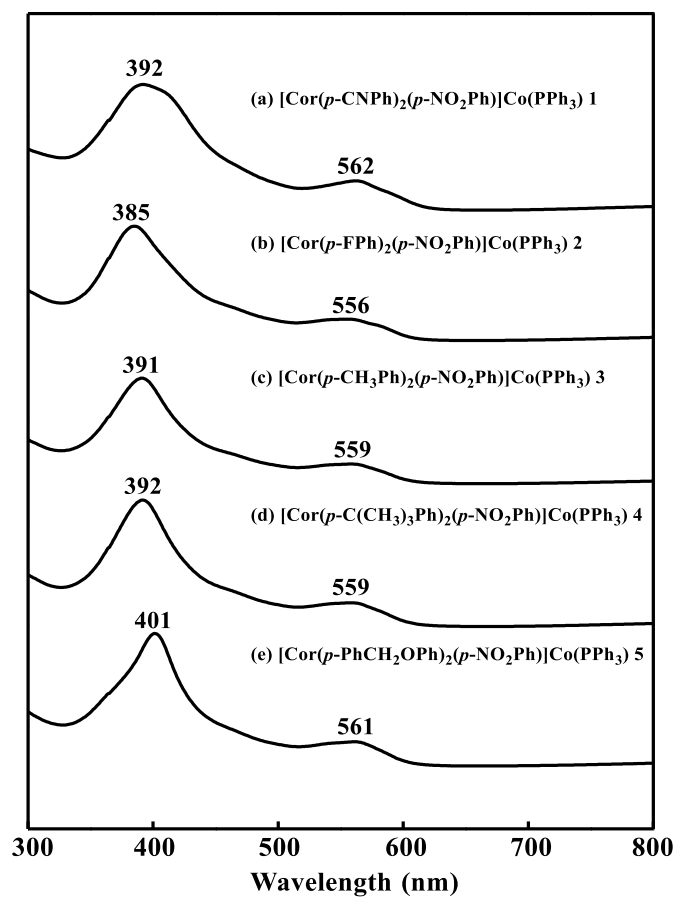


**Fig. S12.** Electronic absorption spectra of compounds  $[\text{Co}(\text{p-RPh})_2(\text{p-NO}_2\text{Ph})]\text{Co}(\text{PPh}_3)$  (1-5) in DMA.

**Table S1.** Electronic absorption data for [Cor(*p*-RPh)<sub>2</sub>(*p*-NO<sub>2</sub>Ph)]Co(PPh<sub>3</sub>) (**1-5**) in CH<sub>2</sub>Cl<sub>2</sub>, DMF and DMA.

Solvent	R	$\lambda_{\max}$ / [nm, $\epsilon \times 10^{-5}$ (L mol <sup>-1</sup> cm <sup>-1</sup> )]		
CH <sub>2</sub> Cl <sub>2</sub>	CN	392 (1.0715)	568 (0.2258)	
	F	386 (1.4355)	553 (0.2792)	
	CH <sub>3</sub>	391 (0.9249)	560 (0.1414)	
	C(CH <sub>3</sub> ) <sub>3</sub>	393 (0.8006)	556 (0.1534)	
	PhCH <sub>2</sub> O	403 (1.7869)	569 (0.2604)	
DMF	CN	396 (0.5440)	563 (0.1398)	628 (0.0720)
	F	387 (0.4811)	548 (0.0885)	620 (0.0297)
	CH <sub>3</sub>	392 (0.8067)	548 (0.1344)	620 (0.0271)
	C(CH <sub>3</sub> ) <sub>3</sub>	390 (1.0095)	556 (0.1647)	623 (0.0309)
	PhCH <sub>2</sub> O	401 (0.8260)	561 (0.1305)	624 (0.0229)
DMA	CN	392 (0.6253)	562 (0.1527)	
	F	385 (0.5651)	556 (0.1094)	
	CH <sub>3</sub>	391 (0.5214)	559 (0.1003)	
	C(CH <sub>3</sub> ) <sub>3</sub>	392 (0.6250)	559 (0.1215)	
	PhCH <sub>2</sub> O	401 (0.6552)	561 (0.1243)	



**Table S2.** Characteristic IR bands ( $\text{cm}^{-1}$ ) of corrole for  $[\text{Cor}(p\text{-RPh})_2(p\text{-NO}_2\text{Ph})]\text{Co}(\text{PPh}_3)$  (**1-5**) with  $2 \text{ cm}^{-1}$  resolution.

CN	F	CH <sub>3</sub>	C(CH <sub>3</sub> ) <sub>3</sub>	PhCH <sub>2</sub> O	Assignment
413w	418w				C-C-C out-of-plane wag of phenyl
458w	459w			457w	Coupling the Pyrrole in plane bending and C-C-C out-of-plane wag of phenyl
499w	499w	499w	499w	499w	Pyrrole in-plane rotation
521s	522s	519s	521s	520s	Pyrrole in plane bending
576w	576w	576w	585w	575w	C(10- <i>meso</i> )-C(Pyrrole) out-of-plane bending
618w	616w	616w	618w	618w	C-C-C in plane deformation of phenyl groups
695s	694s	693s	695s	695s	C-H out-of-plane wag of the Pyrrole
714s	721s	719s	716s	714s	C-H out-of-plane wag of the Pyrrole
747m	747m	747m	742m	746m	C-H out-of-plane wag of the phenyl groups
			749a		C-H out-of-plane wag of the phenyl groups
786m	786m	784m	785m	785m	Pyrrole in-plane deformation
		807m			Pyrrole in-plane bending
820s	820s	820s	821s	822s	Pyrrole in-plane bending
846w	845w	845m	845m	845m	Coupling of Pyrrole stretching and the out of plane C-H wag
881w	880w	880w	881w	880w	C-H in-plane bending of the Pyrrole
985m	986m	985m	985m	985m	Coupling the breathing vibration of the phenyl groups and the corrole skeleton
1013s	1016s	1017s	1018s	1015s	Coupling C-H in plane bending of phenyl groups and porrole breathing
1053m	105s	1052m	1052m	1050m	C-H bending of the Pyrrole
1088w	1088w	1088w	1088w	1088w	C-H in plane bending of the phenyl groups
1109w	1109w	1109w	1109w	1109w	Phenyl groups in plane breathing
1190w	1160s	1184w	1190w		C-H bending of the Pyrrole
				1172s	Ar-O-C stretching ( <i>sym</i> )
	1221s				C-F stretching
1226w	1229s	1226w	1226w	1224w	Coupling of the C(10- <i>meso</i> )-C(phenyl groups) stretching and Pyrrole in plane bending

1249w	1250w	1248w	1249w		Coupling the C(5, 15- <i>meso</i> )-C(phenyl groups) stretching and Pyrrole stretching
				1242s	Ar-O-C stretching ( <i>asym</i> )
1319w	1316m	1318w	1319w	1316w	Pyrrole stretching
1345vs	1343vs	1341vs	1340vs	1342s	Coupling the stretch of pyrrole, C-C stretching and symmetric N=O stretching
1435w	1435m	1435m	1432m	1433m	C-C stretching of the Pyrrole
1507w	1507w	1507s	1506w	1506vs	Coupling of Pyrrole stretching and asymmetric N=O stretching
1521s	1520s	1521s	1520s	1517s	Coupling of the C(5,15- <i>meso</i> )-C(Pyrrole) stretching and Pyrrole in plane bending
	1540w	1540w	1540w	1542w	Coupling of Benzene stretching and asymmetric N=O stretching
1600s	1593m	1593m	1596m	1592m	Benzene stretching
				1601m	Benzene stretching
2225s					C≡N stretching
		2853m	2850m		C-H stretching (-CH <sub>3</sub> -, <i>sym</i> )
				2883br	C-H stretching (-CH <sub>2</sub> -, <i>sym</i> )
		2920s	2921s		C-H stretching (-CH <sub>3</sub> -, <i>asym</i> )
		2953a	2959s		C-H stretching (-CH <sub>3</sub> -, <i>asym</i> )
				2970s	C-H stretching (-CH <sub>2</sub> -, <i>asym</i> )
3062w	3058w	3054w	3058w	3060w	aromatic C-H stretching

<sup>a</sup> Shulder band.

**Table S3.** Half-wave and peak potentials (V vs SCE) for the oxidations and reductions of  $[\text{Co}(\rho\text{-RPh})_2(\rho\text{-NO}_2\text{Ph})]\text{Co}(\text{PPh}_3)$  (**1-5**) in  $\text{CH}_2\text{Cl}_2$  containing 0.1 M TBAP.

Compound	R	Oxidation			Reduction		
		$E_{1/2}(2)$	$E_{1/2}(1)$	$\Delta E(2-1)$	$E_p(1)$	$E_{1/2}(\text{NO}_2\text{Ph})$	$E_p(2)$
<b>1</b>	CN	1.04	0.65	0.39	-0.53	-1.06	-1.53
<b>2</b>	F	0.95	0.57	0.38	-0.66	-1.13	-1.64
<b>3</b>	$\text{CH}_3$	0.93	0.53	0.4	-0.70	-1.15	-1.69
<b>4</b>	$\text{C}(\text{CH}_3)_3$	0.91	0.53	0.38	-0.73	-1.14	-1.70
<b>5</b>	$\text{PhCH}_2\text{O}$	0.87	0.52	0.35	-0.72	-1.14	-1.69

Scan rate 100 mV/s.